LUND UNIVERSITY

Construction and Control of an Educational Lab Process - The Gantry Crane

Larsson, Per-Ola; Braun, Rolf

2008

[Link to publication](#)

Total number of authors:
2

Construction and Control of an Educational Lab Process – The Gantry Crane

Per-Ola Larsson, Rolf Braun

Department of Automatic Control
Lund University
Box 118, SE-211 00 Lund, Sweden
E-mail: {perola.larsson, rolf.braun}@control.lth.se

Abstract: In this paper, we describe the construction and control of a gantry crane that is used in courses at the Department of Automatic Control, Lund university. Two different models of the crane are developed. A thorough example of path following, including on-line time-varying input/state-transformations and LQG control, used in a laboratory exercise is shown together with experimental results. Time-optimal trajectories for position control, with constraints on positions, load angles, and control signals are computed using Modelica and Optimica.

1. INTRODUCTION

Gantry cranes are versatile and come in many different sizes. Their movements are fundamental and consists of hoisting of the load and moving the load pivot point in a plane. Some gantry cranes are used in dock-areas lifting large containers while others might be found in mechanical workshops lifting small engines. They all have at least one thing in common, the load can exhibit pendulum like swinging motions which can result in e.g., damage to load, surrounding environment, or even the gantry crane itself. The dynamics of a gantry crane are non-linear and highly oscillative and constitutes therefore an interesting control problem.

This paper will describe the construction of a laboratory sized gantry crane at the Department of Automatic Control, Lund University. The crane has been used in a teaching environment where circular path following was considered. The implemented control system will be outlined in detail and experimental results will be shown.

A method of computing time-optimal trajectories for a gantry crane using Modelica and Optimica, and resulting trajectories, will be shown. The trajectories can be used as feed-forward and state reference signals.

The outline of the paper is as follows. In Section 2 the construction, including mechanical design, actuators and sensors, are described. Section 3 gives example of control objectives for the gantry crane, while Section 4 shows a thorough example of path following. Future work of the crane is presented in Section 5 and Section 6 gives a brief summary.

2. SYSTEM DESIGN

The gantry crane is constructed to be used in both laboratory exercises and student projects at the Department of Automatic Control, Lund University, but nevertheless, also in research at the department. With this in mind, it is advantageous if the crane can be easily repaired in case of accidents and wear. This requires vast knowledge of the mechanical and electrical construction of the crane. There do exist companies that concentrate on building laboratory processes. Although, a bought in process might be hard to repair for local engineer. The solution to this problem was to build the crane by local design, giving detailed construction knowledge at the same time.

The crane construction was developed with particularly four items in mind. First of all, the different parts of the crane should be low cost. This is mainly due to economical reasons in case of e.g. repairments. Secondly, the constructed gantry crane should be small enough to easily be stored when not in use and also easy to transport in, for instance, case of demonstrations. The third item that was considered was the notion of modularity. There exist an ambition that the different systems used in courses should be build up by modules, both to save space and facilitate maintenance. Replacing a module on a process should amend its behavior in such a way that it can be used in another teaching situation. And fourthly, as discussed above, it should be repairable by local engineers.

2.1 Mechanical Design

An ordinary gantry crane is constructed with two foundation legs on separate rails connected together with an upper rail where a movable trolley is placed. Due to the above discussed constraints on the design, the trolley and the upper rail are in one solid piece. The movement is thus managed by moving the whole upper rail, and the crane body on a lower rail, see Figure 1. The rails are of lengths 1 m and 0.4 m, respectively. Thus, it fits nicely on a normal sized table, with the load hanging on the side. On the back of the upper rail, a hoisting reel is placed together with its drive, giving the opportunity to hoist the load. In the trolley position, i.e., the pivot point of the load, an arm is placed that give measurements of load angles.

2.2 Actuators

For movement along the rail directions, DC motors with gear wheels are used. The motors are of type Faulhaber
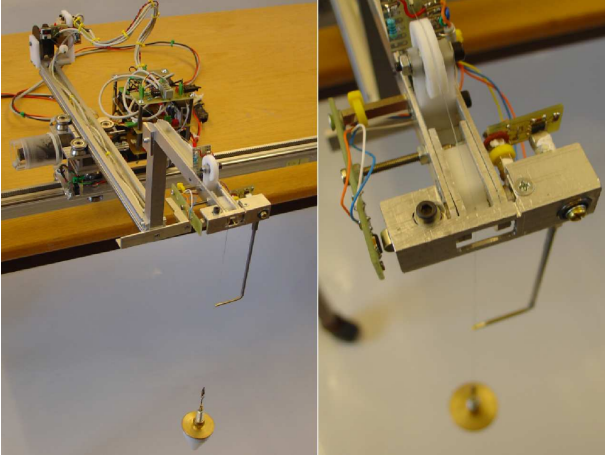
Fig. 1. The laboratory sized gantry crane. The crane can be moved in the directions of the rails and the load can be hoisted.

Fig. 2. Definitions of angles α and β measured by load arm.

3257CR 12V. Hoisting of the load is performed by a smaller type of DC motor, a Fabr Micro Motors HL149 12V. They are both driven by PWM signals generated automatically from MEGA16 micro processors placed on the crane.

2.3 Sensors

The sensors on the gantry crane can essentially be divided into two categories, control sensors and calibration/safety sensors. The control sensors give measurements that are used by control algorithms while the calibration/safety sensors are used for e.g., rail end detection.

Control sensors   The crane is equipped with five control sensors. Two of them are build-in encoders in the rail DC motors. These give high resolution of the position, 512 pulses/6 cm. If desired, these measurements can be used successfully for velocity estimation.

The load hoisting motor do not have a build-in encoder. Instead, an external encoder with a resolution of about 300 pulses/6 cm is mounted on the shaft. Also this measurement can be used for velocity estimation.

Load angles are measured using an arm that can move in two directions, see Figures 1 and 2. The angle from the vertical plane to the plane indicated in the figure, is denote α, while the angle in the plane is denoted β. The arm, made of aluminum, is mounted on the rail using high performance bearings and will therefore not affect the movement of the load in a considerable manner. The load runs through a small hole in the arm, enabling hoisting.

The measurements are obtained by movement of magnetic flux. At the arm, there are two magnets mounted together with two Hall elements, see Figure 1. The Hall elements, incorporated in small IC circuits, outputs a voltage that is, in the ideal case, directly proportional to the magnetic flux direction. This is with the prerequisite that the magnet is mounted above the Hall elements with a certain initial distance and angle. In practice this placement is hard to achieve and since the output voltage is very sensitive to these parameters, the measurements are in practice non-linear functions of the angles. The Hall elements has, in a worst case displacement of a diametral magnet, an
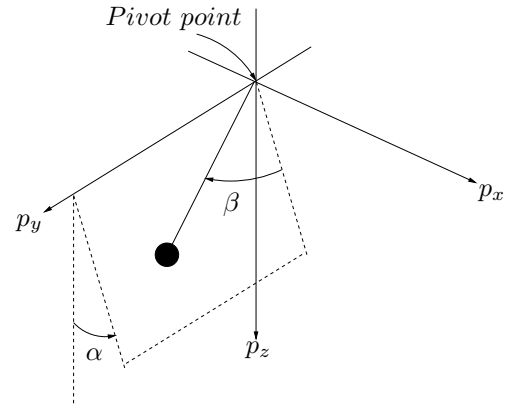
absolute error of about 1°. However, the crane uses axial magnets, which most probably increases the absolute error. Calibration, in form of look-up functions that translate from voltages to radians, is therefore a necessity prior usage. Note that the two magnet/Hall-element sensors must be calibrated separately and will have separate look-up functions. It was found that polynomial functions of order three were sufficient. Typical measurements of the angles can be found in Figure 3, where the load is in an almost circular orbit, and hence the two signals are almost perpendicular. Note that the measurements, in practice, do not have any mentionable noise.
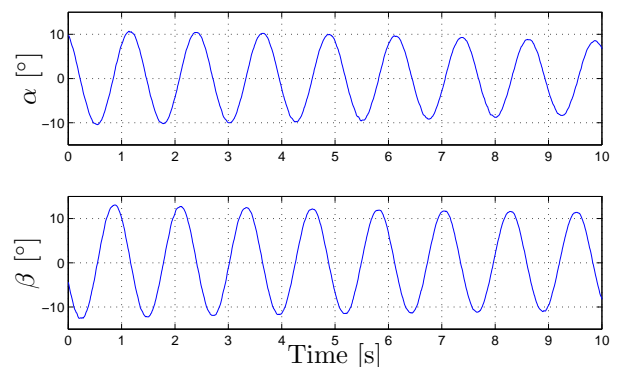

Fig. 3. Example of measurements of $\alpha(t)$ and $\beta(t)$ when the load is in an almost circular orbit.

Calibration/Safety Sensors   In addition to the control sensors, there are four sensors used for safe maneuvering and initialization of the crane. Two sensors, magnetic switches, are placed on the ends of the rails indicating if the crane is at the end point. These can be used for initialization of the crane, e.g., position calibration.

At the hoisting motor and the load pivot point, two magnetic switches are placed to constrain the load length, see Figure 1. Using a small magnet mounted on the load string between the hoisting motor and pivot point, indications are given. These two sensors can be used for load length calibration.

A safety sensor is also placed at the hoisting motor, a switch that removes the drive stage and shuts down the hoisting motor. The switch is set by the magnet on the

string mentioned above. This is needed for protection of the load arm from the load mass if the load is hoisted up too far. Thus, there is a lower bound on how short the load can be, which is the arm length.

An additional precaution is that the cogs on the rails do not go all the way to the rail ends. That is, if the crane goes too far out, the gear weels can not drive the crane. This saves the motors if a faulty control is implemented.

2.4 Micro Processors

To collect data and actuate the motors, Atmel MEGA16 micro-processors are used. These are convenient since they offer important features such as A/D conversion, RS232 communication, PWM signal generation for actuation and a protocol for inter-processor communications, I2C.

The crane is equipped with two of these processors. One actuates and receives measurements from the rail motors, and receives signals from the calibration sensors on the rails. The second actuates, and receive measurements from, the hoisting motor, and take measurements from the calibration/safety sensors concerning the load. This processor acts as the master, and is connected to a PC using common serial communication, (RS232), while the former is the slave in the inter-processor communication.

2.5 Process Modularity

As mentioned in Section 2, one of the constraints in the design of the crane was modularity, which indeed the constructed crane has.

For instance, if the upper rail together with the load is removed, an ordinary pendulum can be mounted. Now, control of an inverted pendulum can be studied and implemented using the existing electronics.

Another example is removal of the crane body and upper rail, and leave only the long rail. This enables other carts to be placed on the rail, for instance, mass-spring systems.

3. CONTROL OBJECTIVES

The gantry crane is versatile in the sense of control objectives. The most common objective is probably downward position damping with references on positions and load length. Another objective is path following, i.e., a specified path is obtained using an optimization procedure. The path can be generated regarding e.g., time-optimal movement with constrained load sway.

4. PATH FOLLOWING - A LABORATORY EXERCISE

The gantry crane has been used successfully in a laboratory exercises in a course at the Department of Automatic Control, Lund University. In the course, which is aimed at multivariable control, LQG is teached. When using LQG, a linear model is of course required. Using the most common control objective, i.e., damping of the downward position of the load, the linearized model becomes essentially two decoupled pendulums which is not suitable in a multivariable course where gain-scheduling is not teached. This also
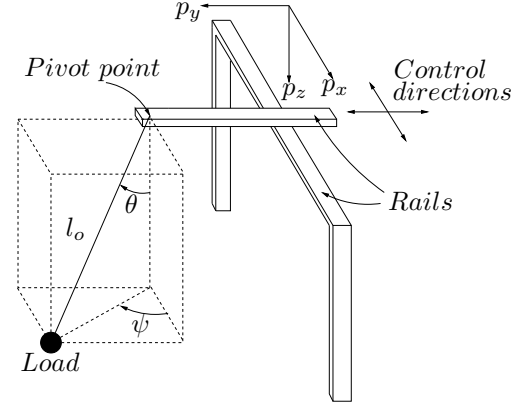

Fig. 4. Crane layout and coordinates. The pivot point of the crane load can be moved in the (p_x, p_y)-plane.

removes the path following objectives where the goal is to keep the load in downwards position.

To have a system that do not have decoupling properties at linearization, the control objective was set to path following with the load mass in a circle with certain radius while, essentially, not moving the crane. The only inputs to be used were the accelerations in the rail directions. The model of this system will have coupled structure after linearization.

4.1 Modeling

Since the control objective is to make the load go in a circular orbit, using spherical coordinates for the load is preferable. However, the rail position expression is simplified using cartesian coordinates. If we introduce, as in Figure 4,

- pivot point $p_x(t)$, $p_y(t)$
- load angles $\theta(t)$ and $\psi(t)$
- load length l_o

we can express the position of the load, $(x_l(t), y_l(t), z_l(t))$, as, see for instance Aston (1999),

$$x_l(t) = p_x(t) + l_o \sin\theta(t)\cos\psi(t)$$
$$y_l(t) = p_y(t) + l_o \sin\theta(t)\sin\psi(t)$$
$$z_l(t) = l_o \cos\theta(t).$$

Note here that we have a fixed length of the load, the hoisting motor will not be used.

By Lagrange mechanics framework, a physical model of the crane can be derived. The kinetic and potential energy of the crane, and the Lagrange function is then given, respectively, by

$$T(t) = \frac{1}{2}M\left(\dot{x}_l^2(t) + \dot{y}_l^2(t) + \dot{z}_l^2(t)\right) + \frac{1}{2}m_1\dot{p}_x^2(t)$$
$$+ \frac{1}{2}m_2\left(\dot{p}_x^2(t) + \dot{p}_y^2(t)\right)$$
$$+ \frac{1}{2}I_1\left(\frac{\dot{p}_x(t)}{r_1}\right)^2 + \frac{1}{2}I_2\left(\frac{\dot{p}_y(t)}{r_2}\right)^2$$
$$+ \frac{1}{2}I_3\left(\frac{\dot{p}_y(t)}{r_3}\right)^2$$
$$V(t) = -Mgz_l(t)$$
$$L(t) = T(t) - V(t) \tag{1}$$

where

M	-	weight of crane load
m_1	-	crane body weight (rail motors, electronics, etc)
m_2	-	bridge weight in p_y-direction including hoisting motor
I_1	-	moment of inertia of p_x-direction motor
I_2	-	moment of inertia of p_y-direction motor
I_3	-	moment of inertia of hoisting motor
r_1	-	radius of the p_x-direction motor pinion
r_2	-	radius of the p_y-direction motor pinion
r_3	-	radius of the hoisting motor pinion

Assuming that the crane is much heavier than the load, which is a reasonable assumption for the constructed crane, the movement of the load will not affect the position of the crane. Thus, we do not need to use the Lagrange function for the generalized coordinates $p_x(t)$ and $p_y(t)$. Instead, we will assume that we have the capability of using the accelerations, i.e., $\ddot{p}_x(t)$ and $\ddot{p}_y(t)$, in these directions as control inputs.

Applying the Lagrange function with the generalized coordinates $\theta(t)$ and $\psi(t)$, i.e.,

$$\frac{d}{dt}\frac{\partial L}{\partial \dot{\theta}(t)} - \frac{\partial L}{\partial \theta(t)} = 0$$

$$\frac{d}{dt}\frac{\partial L}{\partial \dot{\psi}(t)} - \frac{\partial L}{\partial \psi(t)} = 0$$

we get the following equations of motions for the gantry crane

$$2l\dot{\theta}\dot{\psi}\cos\theta + l\ddot{\psi}\sin\theta - u_x \sin\psi + u_y \cos\psi = 0 \quad (2)$$

$$g\sin\theta + l\ddot{\theta} - \frac{1}{2}l\dot{\psi}^2\sin 2\theta + u_x \cos\theta\cos\psi \quad (3)$$
$$+ u_y \cos\theta\sin\psi = 0$$

where $u_x(t)$ and $u_y(t)$ are accelerations in the corresponding rail directions.

We can see that, since a specified radius of the load orbit corresponds to a specified θ, the control authority will depend on ψ.

4.2 Linear Time Varying Model

The LQG control structure requires a linear model. Linearizing around the desired trajectory, translating the specified radius to an angle θ_o yields the following trajectory,

$$\begin{pmatrix} p_y(t) \\ \dot{p}_y(t) \\ p_x(t) \\ \dot{p}_x(t) \\ \theta(t) \\ \dot{\theta}(t) \\ \psi(t) \\ \dot{\psi}(t) \\ u_x(t) \\ u_y(t) \end{pmatrix} = \begin{pmatrix} 0 \\ 0 \\ 0 \\ 0 \\ \theta_o \\ 0 \\ \omega_o t \\ \omega_o \\ 0 \\ 0 \end{pmatrix}$$

where ω_o is the rotational velocity of the load. Note that, for a circular orbit of the load, the angle θ_o and ω_o are related as

$$\omega_o = \sqrt{\frac{g}{l_o \cos\theta_0}}$$

where l_o is desired length of load. Thus, essentially, the orbit is defined by only θ_o.

A straight forward linearization around this trajectory results in the following time varying system where the states are deviations from the trajectory, i.e.,

$$\begin{pmatrix} \Delta\dot{p}_y \\ \Delta\ddot{p}_y \\ \Delta\dot{p}_x \\ \Delta\ddot{p}_x \\ \Delta\dot{\theta} \\ \Delta\ddot{\theta} \\ \Delta\ddot{\psi} \end{pmatrix} = \begin{pmatrix} 0 & 1 & 0 & 0 & 0 & 0 & 0 \\ 0 & 0 & 0 & 0 & 0 & 0 & 0 \\ 0 & 0 & 0 & 1 & 0 & 0 & 0 \\ 0 & 0 & 0 & 0 & 0 & 0 & 0 \\ 0 & 0 & 0 & 0 & 0 & 1 & 0 \\ 0 & 0 & 0 & 0 & s_1 & 0 & s_2 \\ 0 & 0 & 0 & 0 & 0 & s_3 & 0 \end{pmatrix} \begin{pmatrix} \Delta p_y \\ \Delta\dot{p}_y \\ \Delta p_x \\ \Delta\dot{p}_x \\ \Delta\theta \\ \Delta\dot{\theta} \\ \Delta\dot{\psi} \end{pmatrix}$$

$$+ \begin{pmatrix} 0 & 0 \\ 0 & 1 \\ 0 & 0 \\ 1 & 0 \\ 0 & 0 \\ -b\cos\psi(t) & -b\sin\psi(t) \\ a\sin\psi(t) & -a\cos\psi(t) \end{pmatrix} \begin{pmatrix} \Delta u_x \\ \Delta u_y \end{pmatrix},$$

where $\psi(t) = \omega_o t$ and

$$s_1 = \omega_o^2 \cos(2\theta_o) - \frac{g}{l}\cos\theta_o \qquad a = \frac{1}{l\sin\theta_o}$$

$$s_2 = \omega_o \sin 2\theta_o \qquad b = \frac{\cos\theta_o}{l}$$

$$s_3 = -2\omega_o \cot\theta_o.$$

Note that the deviation from ψ do not occur as a state. It can be removed since no other state depend on it. It might also be physically impossible for the load to follow $\omega_o t$ exactly since it will depend on experiment start time.

The angles $\theta(t)$ and $\psi(t)$ can be calculated from the measurements as

$$\theta(t) = \arccos\left(\cos\alpha(t)\cos\beta(t)\right) \quad (4)$$

$$\psi(t) = \arctan\left(\frac{\tan\beta(t)}{\sin\alpha(t)}\right) \quad (5)$$

Note that ψ is undefined if $\sin\alpha = 0$, i.e., it is discontinuous in π intervals. It can easily be reconstructed to a continuous signal by calculating a running offset on the angle.

4.3 State and Control Signal Transformations

Since we need a linear time invariant system to design the controller, introduce a coordinate system that rotates with the load. The model can be transformed into these coordinates using the time dependent input transformation matrix $P(\psi(t))$ and state transformation matrix $T(\psi(t))$,

$$P(\psi(t)) = \begin{pmatrix} \cos\psi(t) & -\sin\psi(t) \\ \sin\psi(t) & \cos\psi(t) \end{pmatrix} \quad (6)$$

$$T(\psi(t)) = \text{blockdiag}\left(T_{11}(\psi(t)), I_3\right) \quad (7)$$

where the sub matrix

$$T_{11}(\psi(t)) = \begin{pmatrix} 0 & -\sin\psi(t) & 0 & -\cos\psi(t) \\ \cos\psi(t) & 0 & -\sin\psi(t) & 0 \\ \sin\psi(t) & 0 & \cos\psi(t) & 0 \\ 0 & \cos\psi(t) & 0 & -\sin\psi(t) \end{pmatrix}$$

Applying the transformations as

$$\Delta u_{xy}(t) = P(\psi(t))u(t) \qquad (8)$$
$$x(t) = T(\psi(t))\Delta x(t) \qquad (9)$$

where $\Delta u_{xy}(t)$ and $\Delta x(t)$ are the control signal and state vector, respectively, in the time varying linear system, gives a time invariant system

$$\dot{x}(t) = \underbrace{\begin{pmatrix} 0 & 0 & 0 & -\omega_o & 0 & 0 & 0 \\ 0 & 0 & -\omega_o & 1 & 0 & 0 & 0 \\ -1 & \omega_o & 0 & 0 & 0 & 0 & 0 \\ \omega_o & 0 & 0 & 0 & 0 & 0 & 0 \\ 0 & 0 & 0 & 0 & 0 & 1 & 0 \\ 0 & 0 & 0 & 0 & s_1 & 0 & s_2 \\ 0 & 0 & 0 & 0 & 0 & s_3 & 0 \end{pmatrix}}_{A} x(t) + \underbrace{\begin{pmatrix} -1 & 0 \\ 0 & 0 \\ 0 & 0 \\ 0 & 1 \\ 0 & 0 \\ -b & 0 \\ 0 & -a \end{pmatrix}}_{B} u(t).$$
$$(10)$$

where ω_o is the rotational velocity and s_i, a and b are the constants defined above.

This system, with as above defined A and B matrices, will be used in the forthcoming LQG design.

The eigenvalues of the system matrix A are

$$\lambda_{1,2} = \pm i\omega_o \qquad \lambda_{3,4} = \pm i\omega_o$$
$$\lambda_{5,6} = \pm i\sqrt{s_1 + s_2 s_4} \qquad \lambda_7 = 0.$$

We thus have a highly oscillative system to control.

4.4 Control Structure

The control structure is hierarchical, two local loops concerning motor control and one outer for the over all control objective. Thus, the outer loop will generate reference signals for the local motor loops.

The modelling assumes that we can control the accelerations in the rail directions. Since we do not have direct measurements of the accelerations and we not have direct access to the currents in the DC motors, a simple solution is to control the velocity in the different rail directions instead. If this control is fast enough, reference trajectories can be generated by integrating the acceleration reference. In the outer loop, we will control the velocities, preventing drift in the reference generating integrator. The velocities are estimated using ordinary first order derivative filters, i.e,

$$G_{\dot{p}_i}(s) = \frac{s}{\frac{1}{30}s + 1}, \qquad i = x, y$$

that are sampled with period $h = 10$ ms. The velocities are controlled by PI controllers and friction compensators using the signs of the velocity references,

$$u_{motor,i}(t) = u_{PI,i}(t) + \alpha_i \cdot \text{sgn}(v_{ref,i}(t))$$
$$v_{ref,i}(t) = \frac{1}{s}u_i(t), \qquad i = x, y$$

where $u_i(t)$ are the acceleration references generated by the outer loop, i.e, the control signals in the linear time-invariant model in Eq. (10).

Typical values of the PI controllers parameters are

$$K = 3 \qquad T_i = 0.15$$

when using normalized motor control signals, $u_{motor,i}(t) \in [-1,1]$ and measurements/references in SI-units.

The outer controller is an ordinary LQG controller, i.e., a controller that minimizes

$$J = \int_0^\infty \left(x^T(t)Q_1 x(t)dt + u^T(t)Q_2 u(t) \right) dt$$

with the structure
$$\dot{\hat{x}}(t) = A\hat{x}(t) + Bu(t) + K(y(t) - C\hat{x}(t))$$
$$u(t) = -L\hat{x}(t)$$

The measurements used in the Kalman filter are x_2, x_3, x_5. These are the positions Δp_x and Δp_y and the angle $\Delta\theta$ transformed using sub matrices in $T(\psi(t))$, see Eqs. (7) and (9). Prior the control signal $u(t)$ is applied it is transformed using $P(\psi(t))$, see Eqs. (6) and (8). Thus, the measurement of ψ is necessary for transformations.

Due to simplicity, only diagonal weight and noise covariance matrices were considered in the LQG design.

4.5 Experimental results

Design and evaluation of LQG controllers were performed in Matlab/Simulink using a model of the crane, with local motor-loops modelled as first order systems with an experimentally estimated time constant. The switch to hardware was straightforward, no retuning had to be done.

In the experimental setup, desired θ was set to 30°. The crane was initialized to the position $p_x(t) = p_y(t) = 0$ with the load following an approximate circular orbit of about 12°, see Figure 5. As the controllers were activated, the load is driven close to the desired trajectory. Only a small movement and acceleration of the crane is required, about 5 cm in each rail direction and less than 1.5 m/s², respectively, see Figure 6.

A load disturbance was introduced at approximately 14 s, an object interrupts the circular movement yielding θ to decrease to about 5°.

One can see that the load angle is not constant, which is due to many factors. First of all, $\theta(t)$ is computed using two measurements, see Eq. (4), which are separately computed using non-linear look-up functions. In addition to that, the Hall elements might have errors as mentioned in Section 2.3. One must also take into consideration that the rail drives are implemented using gear wheel, which gives a certain amount of backlash that is not compensated for.

5. FUTURE WORK

As mention in Section 3, the probably most common control objective is downwards damping with reference on position. A control strategy that can be used in this case is feed-back and an off-line trajectory optimization. The trajectory is used as feed-forward and reference signal to states of the crane. The feed-back is then used on the state-errors.

Below, time-optimal trajectories for positioning of the crane, with constraints on both load angles, crane velocities, and control signals, will be derived using Modelica and Optimica. The trajectories are supposed to be used in future work, being implemented on the real gantry crane using Matlab/Simulink.
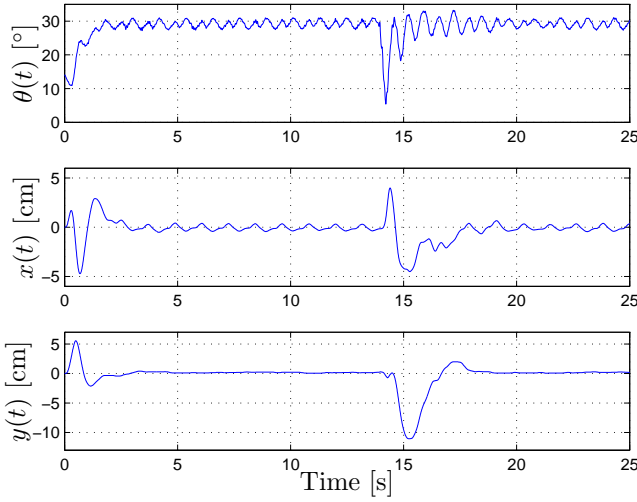
$$\frac{d}{dt}\frac{\partial L}{\partial \dot{\alpha}(t)} - \frac{\partial L}{\partial \alpha(t)} = 0$$
$$\frac{d}{dt}\frac{\partial L}{\partial \dot{\beta}(t)} - \frac{\partial L}{\partial \beta(t)} = 0$$

This gives the equations of motions now expressed in $\alpha(t)$ and $\beta(t)$, i.e.,

$$u_x \cos\alpha + l\ddot{\alpha}\cos\beta + g\sin\alpha + 2l\dot{l}\dot{\alpha}\cos\beta - 2l\dot{\alpha}\dot{\beta}\sin\beta = 0 \quad (11)$$

$$l\ddot{\beta} + g\cos\alpha\sin\beta + 2\dot{l}\dot{\beta} + l\dot{\alpha}^2\sin\beta\cos\beta$$
$$+ u_y\cos\beta - u_x\sin\beta\sin\alpha = 0 \quad (12)$$

The control signals in this system are u_i, $i = x, y, l$, i.e., the accelerations in along the rails and hoisting direction.

The optimization problem is now to find control signals u_i such that we fulfill constraints on e.g., maximum angles, velocities, and positions. Using Modelica, it is easy to simulate the equations of motions. By Optimica, which is an extension of Modelica with language constructs which enables formulations of optimization problems based on Modelica models, the optimization problem can be solved numerically. See for instance Åkesson (2007) for more information on Optimica.

The movement of the crane considered here will be positioning. From the initial state of positions, velocities, and control signals equal to zero, and with load length 0.4 m, move the crane 0.8 m and 0.3 m, in the p_x and p_y direction, respectively. At the end, the load length should be 0.4 m.

The trajectories will be time-optimal, with additional constraints on positions and control signals. End constraints on velocities and control signals are added for the crane to be, and stay, at rest when desired position is reached. Limits on $|\dot{u}_i(t)|$ and $|\ddot{u}_i(t)|$ are used, otherwise the control signals in the optimal solution will be of bang-bang character or have rapidly changing derivatives that might not be feasible in practice. The optimization problem can be posed as follows, where t_f denotes end time,

$$\min_{u_x, u_y, u_l} \int_0^t 1\, dt \quad (13)$$

subject to
Eqs. $(11) - (12)$

$$0 \leq x(t) \leq 0.8$$
$$0 \leq y(t) \leq 0.3$$
$$0.2 \leq l(t) \leq 0.6$$

$$|\alpha(t)| \leq 0.3, \quad |\beta(t)| \leq 0.15$$

$$|u_i(t)| \leq 2,\ |\dot{u}_i(t)| \leq 5,\ i = x, y$$
$$|u_l(t)| \leq 1,\ |\dot{u}_l(t)| \leq 3$$
$$|\ddot{u}_j(t)| \leq 100,\ j = x, y, l$$

$$p_x(t_f) = 0.8, \quad \dot{p}_x(t_f) = 0$$
$$p_y(t_f) = 0.3, \quad \dot{p}_y(t_f) = 0$$
$$l(t_f) = 0.4, \quad \dot{l}(t_f) = 0$$
$$\alpha(t_f) = 0, \quad \dot{\alpha}(t_f) = 0$$
$$\beta(t_f) = 0, \quad \dot{\beta}(t_f) = 0$$
$$u_k(t_f) = 0,\ \dot{u}_k(t_f) = 0,\ k = x, y, l$$

Fig. 5. Load angle $\theta(t)$ and crane position $x(t)$, $y(t)$, in experiments on crane. The references were 30°, 0 m and 0 m, respectively. A disturbance is entered at 14 s.
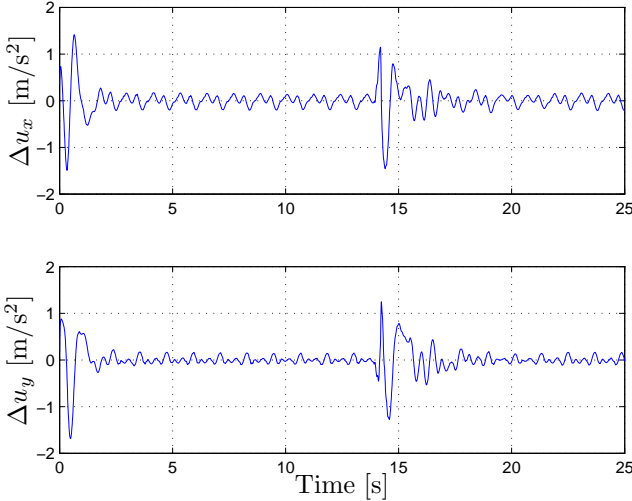
Fig. 6. Rail accelerations Δu_x and Δu_y in experiments on crane. A disturbance is entered at 14 s.

5.1 Time-Optimal Control

To generate optimal trajectories a model is needed. However, the model in Eqs. (2)-(3) can not be used since it is singular in the downward position, ψ is not well defined. By instead using the angles defined in Figure 2, we can express the position of crane load as, see e.g., Aston (1999)

$$x_l(t) = p_x(t) + l(t)\cos\beta(t)\sin\alpha(t)$$
$$y_l(t) = p_y(t) + l(t)\sin\beta(t)$$
$$z_l(t) = l(t)\cos\beta(t)\cos\alpha(t)$$

Note here that the length of the load is not constant but rather a function of time compared to the model used in Section 4, since we now will use the hoisting mechanism on the crane.

Using the Lagrange function defined in Eq. (1) with the above definition of load position, we can calculate
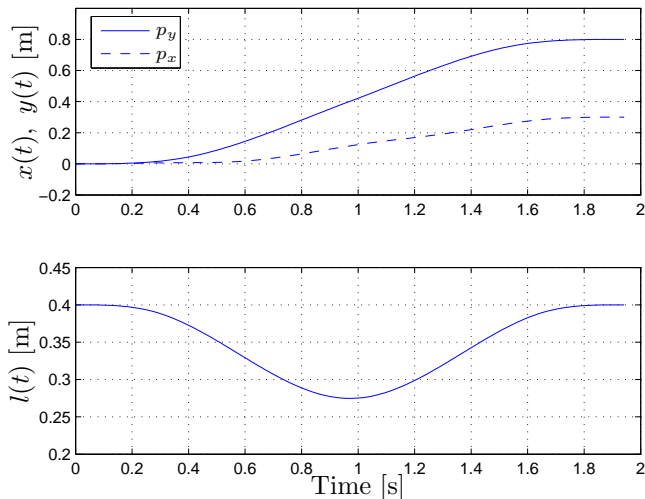
Fig. 7. Positions $p_x(t)$ and $p_y(t)$ and load length $l(t)$ when using time-optimal trajectories.
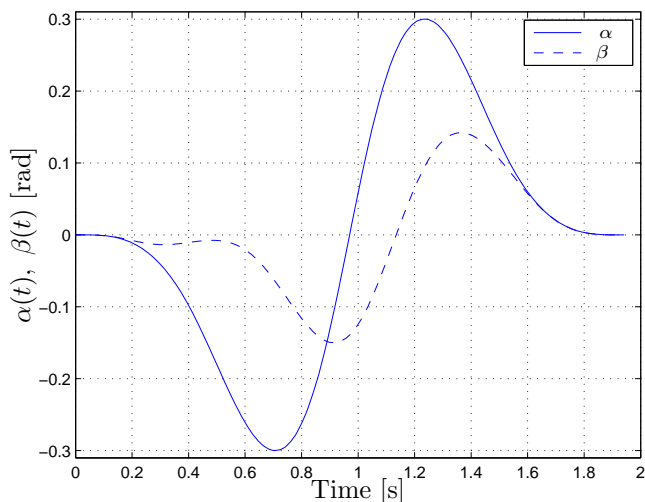

Fig. 8. Angles $\alpha(t)$ and $\beta(t)$ when using time-optimal trajectories.

Solving the considered optimization problem using Optimica results in the position and load length trajectories in Figure 7 and load angles in Figure 8. The control signals $u_x(t)$, $u_y(t)$ and $u_l(t)$, i.e., the accelerations of the motors, are found in Figure 9. The movement time is about 1.94 s. Constraints are active on both the angles and the control signals.

No sharp edges are found in the control signals due to the constraints on $\dot{u}_i(t)$ and $\ddot{u}_i(t)$. If these constraints are removed, the trajectory length will be approximately 1.5 s.

The generated trajectories will in future work be used as feed-forward control signals and state reference signals.

6. SUMMARY

In this paper we have considered the construction of a laboratory sized gantry crane. Two different non-linear
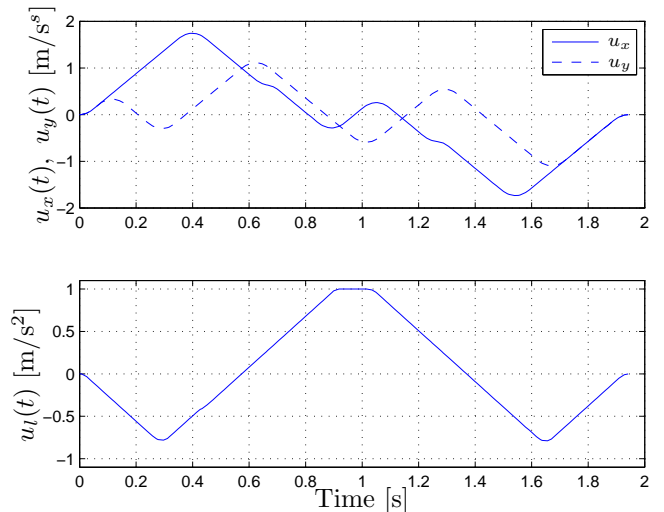

Fig. 9. Control signals $u_x(t)$, $u_y(t)$ and $u_l(t)$ when using time-optimal trajectories.

models of the gantry crane has been derived. A path following example, with on-line time-varying state and control signal transformations and LQG control, has been thoroughly discussed and successful experimental results were shown.

Time-optimal trajectories has been derived using Modelica and Optimica and will in future work be used in an experimental situation.

7. ACKNOWLEDGEMENT

REFERENCES

Johan Åkesson. *Tools and Languages for Optimization of Large-Scale Systems.* PhD thesis, Department of Automatic Control, Lund University, Sweden, November 2007.

P.J. Aston. Bifurcations of the horizontally forced spherical pendulum. *Computer Methods in Applied Mechanics and Engineering*, 170(3-4):343–353, 1999.